Highlights

Human Walking Analysis in a Random Walk Framework

- Analysis of human walk movement using a combined deterministic-stochastic model within a continuous time random walk framework
- Experimental analysis of human walk trajectories simulating movement combinations of the Laban *Effort* subcategories
- Analysis of random time intervals and simulation of human walk trajectories within the Laban *Effort* framework

Human Walking Analysis in a Random Walk Framework

ARTICLE INFO

Keywords:
Laban Movement Analysis
Random Walk
Stochastic Model

ABSTRACT

In this paper, we analyze the human walk movement via a combined deterministic-stochastic model built on top of a random walk framework. By adopting the Laban *Effort* subcategories to investigate different movement classes, we discuss how stochastic and deterministic forces combine to determine the act of moving and relate the stochastic component to the times at which we can observe a movement change. Major elements of our study are the analysis of random times when there is a walk movement change, the construction of a distribution (waiting time distribution), and the implementation of a dichotomic stochastic force. In particular, we report the observed walk trajectories obtained via an experimental analysis performed in collaboration with a group of volunteers to show, to some degree, the relationship between their walks and the measured relevant random times. Finally, we present our model results via simulated trajectories of a virtual character.

1. Introduction

Human movement analysis is a subject of great attention within the scientific community of several different areas, [1], [2], [3], [4]. Among several studies, some of them analyze changes in human movement. For example, one study examines energy expenditure, acceleration, and body tilt angle during falling [5]. In sports-related disciplines, researchers compare step kinematics, joint angles, and muscle activation during change of direction maneuvers [6]. However, only a few studies have focused on the duration of movements and provided an association between human movement features and the observed times [7], [8]. Furthermore, while kinematic analysis can provide insights into velocity and acceleration of movement [9], [10], [11] it does not offer a clear description of the statistical nature of the time interval sequences between observable movement changes. As discussed in the paper, we believe that the analysis of the times at which we can observe a change in human movement can contribute towards a deeper understanding of the human movement. This aspect is further detailed throughout the paper, where we show that the analysis of a human walking ultimately reduces, in our model, to the analysis of variations in measurable random quantities, such as random time interval and random step lengths. Specifically, we aim to utilize these quantities to propose a novel quantitative combined deterministic-stochastic model associated with the movement classes described by the Laban *Effort* framework within the Laban Movement Analysis (LMA).

LMA is a pillar among movement analysis systems [12], [13], [14]. Developed by the dancer and choreographer Rudolph Laban, [15], LMA focuses on the process of the human movement, providing a tool for perceiving and describing the motion [16]. LMA is a very multidisciplinary powerful means suitable at describing the structural characteristics and expressions of human motion, as a result of the interaction among the mover, itself, the others, and the environment [17], [18], [19].

Along with the LMA description, we present a novel approach aimed at taking into account the random times when a walk movement changes, i.e., when a random quantity associated with the observed movement changes and extracting the time interval distribution characterizing human walking. The idea of a time distribution suggests the use of a stochastic model. Specifically, we will show how to combine deterministic and stochastic components for human movement description within the Laban *Effort* subcategories [15], as well as to simulate a virtual character expressing different movements.

The structure of the paper is as follows: in Sec. 2, we describe the Laban framework, showing some specific movements in association with the bipolar characteristics of the *Effort* subcategories. In Sec. 3, we present our model, discussing the conceptual basis and the role of the main parameters. Section 4 describes the experimental analysis and the adopted procedure to instruct the volunteers before each walk. In Sec. 5, we show how to extract the model parameters from the observed trajectories and measured random times. In Sec. 6, we report the simulated trajectories of a virtual character for different combinations of the *Effort* subcategories, and, finally, we present our conclusions.

2. The Laban *Effort* framework and its subcategories

According to the framework proposed by Irmgard Bartenieff [16], the LMA defines four main categories: *Body*, *Space*, *Shape*, and *Effort*. The *Body* category describes how the movement is organized and sequenced in the body. It describes "what is moving", how the body organizes itself. The *Space* category describes "where the body moves", how the mover directs her/his attention onto the environment. *Body* and *Space* are

ORCID(S):

Figure 1: The frame sequence (a), (b), and (c) exhibits a strong *weight* movement, while the frame sequence (d), (e), and (f) shows a light *weight* movement.

Figure 2: The frame sequence (a), (b), and (c) exhibits a direct *space* movement, while the frame sequence (d), (e), and (f) shows an indirect *space* movement.

kinematic features and describe the structural characteristics of the movement [20].

On the other hand, the *Shape* and *Effort* categories are more relevant to the qualitative aspects of the movement [21]. The *Shape* looks at the change of the form of the body, about self or to others, "toward where" the body is changing its shape, as a bridge between *Body* and *Space*. Finally, the *Effort* reflects the attitude towards the movement, "how the body moves". The *Effort* manifests through four different bipolar factors [22]: *weight*, *space*, *time*, and *flow*. The *weight* can be strong (Fig. 1 - frames (a), (b), and (c)) or light (Fig. 1 - frames (d), (e), and (f)), as well as the *space* direct (Fig. 2 - frames (a), (b), and (c)) or indirect (Fig. 2 - frames (d), (e), and (f)), the *time* sudden (Fig. 3 - frames (a), (b), and (c)) or sustained (Fig. 3 - frames (d), (e), and (f)), and the *flow* free (Fig. 4 - frames (a), (b), and (c)) or bound (Fig. 4 frames (d), (e), and (f)).

The *weight* primarily relates to one's relationship with Earth's gravity, although it has not to be associated with the body weight per se. A strong *weight* indicates a body more inclined to fall in gravity. A direct *space* is characterized by a focused inner impulse to move, where the movement expresses an intention to follow a straight line towards a specific point, while an indirect *space* exhibits a more diffuse and broad sense of attention to the surrounding environment.

The *time* is concerned with the attitude toward how (sudden or sustained) the person approaches the movement. Thus, the *time* has not to be associated with the time duration of the action but is related, in our model, to the time to wait for the next observable movement change. Finally, the *flow* characterizes the control of the movement during the action; in our discussion, it indicates a sort of memory of the movement sequence.

Looking at Fig. 1, frames (a), (b), and (c), it is apparent how the body is closer to the ground for the strong *weight* movement, in comparison with the light *weight* movement. Thus, stronger/lighter weight movements imply larger/smaller energy dissipation. A simulation of such a concept is shown in Fig. 1, and analogously for the other subcategories in Figs. 2-4. Consecutive frames are separated by about 0.15 s for

Figure 3: The frame sequence (a), (b), and (c) exhibits a sudden *time* movement, while the frame sequence (d), (e), and (f) shows a sustained *time* movement.

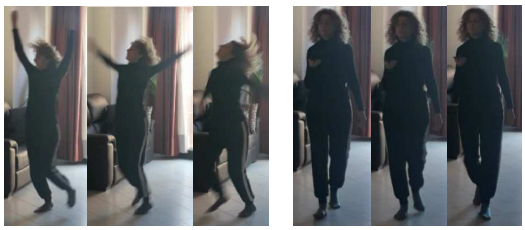

Figure 4: The frame sequence (a), (b), and (c) exhibits a free *flow* movement, while the frame sequence (d), (e), and (f) shows a bound *flow* movement.

all Figs. 1-4. In all cases, movements are performed by an expert in body language and LMA. Although these images cannot represent the whole complexity of the corresponding movements, it is possible to get the bipolar characteristics of the four subcategories considered.

From the frame sequence (a), (b), and (c) of Fig. 2, we can observe how the person moves toward an expected goal while a sense of more indulgence in the space appears in the other case.

The frame sequence (a), (b), and (c) of Fig. 3 simulate a relatively higher urgency in the movement process while the body seems to indulge in the time in the other sequence.

From Fig. 4, frame sequence (a), (b), and (c), it is apparent how the movement with free *flow* more

randomly interests the space outside the body of the person, while the bound *flow* sequence obliges the body to move within a more controlled space. As we will further discuss in our model, a bound *flow*, implies a sort of body memory, such as the gesture of a twirling dancer requires high movement control, as the result of a long body training.

3. Stochastic Model

As known from the literature, Brownian motion can be described within random walk theory as a stochastic process in which a particle moves randomly to the nearest point at equal time intervals. The random walk represents a generalization of the Brownian motion, and it finds applications in many disciplines, among which mathematics, statistical physics, economy, sociology, network science, [23, 24, 25, 26].

The idea of adopting a random walk framework to implement our conjecture arises from visualizing the very classic example of the drunk's walk, in association with the unpredictable component of human motion. In more detail, the drunk person does not know where he/she is going, and flips a coin at each step to decide whether to go forward or back, right or left; this physically pictures the basic concept of a random walk Finally, the position of the drunk person after n "decisions" is a random variable. More specifically, for a continuous time random walk, the walker tosses the coin at random times extracted by a time distribution, and, as a consequence, the movement changes happen in a random time sequence.

The proposed model implements a deterministic force in association with the direct *space* component, while models *weight* via a friction coefficient to simulate the energy spent against the gravitational field during motion. The *time* is characterized by a waiting time distribution. A stochastic force characterizes the free *flow* component. It is, however, important to point out that *space* and *weight* are not deterministic per se. Indeed, the randomness of *time* and *flow* reflects into *space* and *weight*, as well as the deterministic component of the movement associated with *space* and *weight* affects the other two subcategories. The adopted strategy implements a combined deterministic-stochastic process. Finally, all the parameters can be identified by observing human movements, as will be discussed in the following.

Let us now define $\mathbf{F}$ as a force that can exert an action to move the human body, and let us write $\mathbf{F}$ as the sum of the two contributions:

$$\mathbf{F} = \mathbf{F}_d + \mathbf{F}_r \tag{1}$$

where the first term, $\mathbf{F}_d$, is the deterministic force and $\mathbf{F}_r$ represents the stochastic term. The deterministic component induces motion toward a stable objective, while the stochastic force contributes to a random fluctuation of the movement from a stable trajectory. Human walks, characterized by higher and dominating values of $\mathbf{F}_d$, are thus an expression of direct *space* from a point A toward a point B, while higher values of $\mathbf{F}_r$ imply a random walk, an indirect *space*. On the other hand, higher values of $\mathbf{F}_r$ can also be interpreted as an expression of free *flow*, as it will become apparent from our discussion. The stochastic force is modeled as a dichotomic process in our description. As a consequence, $\mathbf{F}_r$ fluctuates between the constant values $\pm\mathbf{F}_0$, with a distribution density of time durations of the two states extracted from a time distribution $\psi(t)$. Thus, the random part can be sketched as a series of "stop and go" separated by a random time interval extracted from $\psi(t)$.

Let us now introduce the force $\beta\mathbf{v}$, which is representative of a friction effect, i.e., in our model, of the energy dissipation to exert the motion, or, in other words, of the energy spent for moving against the gravitational field. This term includes the *weight* in our scheme, and higher/lower energy dissipation implies greater/smaller values of the friction coefficient β. Thus, we have:

$$m\frac{d\mathbf{v}}{dt} = -\beta\mathbf{v} + \mathbf{F} \tag{2}$$

where $\beta\mathbf{v}$ is the phenomenological quantity representing the *weight*. At a first discussion, we can simplify (2) assuming the term $m\,d\mathbf{v}/dt$ to be negligible for our analysis, thus writing:

$$\beta\mathbf{v} = \mathbf{F}, \quad \Rightarrow \mathbf{v} = \frac{\mathbf{F}}{\beta} = \frac{\mathbf{F}_d}{\beta} + \frac{\mathbf{F}_r}{\beta} \equiv \mathbf{v}_d + \mathbf{v}_r \tag{3}$$

Indeed, a negligible $m\,d\mathbf{v}/dt$ assumption means that the stochastic velocity component $\mathbf{v}_r$ does not vary between two consecutive velocity changes. The conditions for neglecting the acceleration are discussed in detail by Smoluchowski [27], [28]. In more detail, according to such an assumption, the times for the velocity changes are short compared to the time intervals between two consecutive changes. In other words, under the Smolochowski conditions, the motion is considered to be substantially uniform between two consecutive changes. Such an approximation should be possibly removed for a person walking in a crowded space.

As a consequence, $\psi(t)$ expresses the time during which the velocity $\mathbf{v}_r$ keeps the value $+\mathbf{v}_0$ or $-\mathbf{v}_0$. More sudden *time* are expected to be associated with more rapid changes, i.e., smaller average time intervals.

$$\mathbf{v}_r = \mathbf{v}_0\xi(t) \tag{4}$$

where $\xi(t) = \pm 1$ represents a random fluctuating quantity, thus, generating the values $\pm \mathbf{v}_0$. We may then rewrite (3) as:

$$\mathbf{v} = \frac{d\mathbf{r}}{dt} = \mathbf{v}_d + \mathbf{v}_r, \Rightarrow \frac{d}{dt}(\mathbf{r} - \mathbf{v}_d t) = \mathbf{v}_0 \xi(t) \quad (5)$$

where $\mathbf{r}$ is the position of the walker. Thus, (5) describes a random walker moving with a constant velocity for a random time τ_1, then changing velocity for a time τ_2, and then again for a time $\tau_3, \ldots, \tau_n$.

As we will see in the next Section, the experimental analysis leads us to adopt a Poissonian distribution, with the exponent coefficient being a phenomenological parameter. Thus, the random times are extracted from a Poissonian distribution $\psi(t) = \gamma \exp[-\gamma t]$, where the parameter $1/\gamma$ represents the average time to make a decision.

$$P(x,t) = \frac{1}{2}\exp\left[-\gamma t\right]\left[\delta\left(f_0 t - |x - f_d t|\right) + \frac{\gamma}{f_0} \times \left(I_0\left[\gamma\sqrt{t^2 - \left(\frac{x - f_d t}{f_0}\right)^2}\right] + \frac{t I_1\left[\gamma\sqrt{t^2 - \left(\frac{x-f_d t}{f_0}\right)^2}\right]}{\sqrt{t^2 - \left(\frac{x-f_d t}{f_0}\right)^2}} \right) \theta\left(f_0 t - |x - f_d t|\right)\right], \quad (6)$$

is the probability distribution to find the walker at the coordinate x when the walker started at the origin, $P(x,0) = \delta(x)$. Here $I_n(z)$ is the modified Bessel function of the first kind and $\delta(t - |x|)$ is Dirac's delta, a function that represents the walkers that never changed their velocity.

According to statistical theory, the described process is expected to recover a Gaussian diffusion process for a time sufficiently large, or, equivalently, for a relatively high value of γ.

$$P(x,t) \approx \sqrt{\frac{\gamma}{2\pi t}} \exp\left[-\frac{\gamma}{2}\frac{(x - f_d t)^2}{t}\right]. \quad (7)$$

At a first analysis, depending on the intensity of the random process, short average times to make a decision can interpret a sense of urgency, as well as an unbound *flow*. In all cases, such a condition indicates something far from the expression of a well-controlled movement sequence.

On the other hand, relatively small values of γ compared to the intensity of the stochastic process can be more related to sustained *time*, or bound *flow*.

Besides, in the limit of $\gamma \to 0$, the motion equation writes as:

$$\frac{1}{f_0^2}\frac{\partial^2}{\partial t^2}P(x,t) + \frac{\gamma}{f_0^2}\frac{\partial}{\partial t}P(x,t) = \frac{\partial^2}{\partial x^2}P(x,t). \quad (8)$$

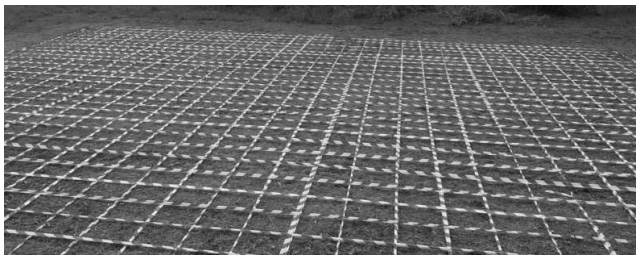

Figure 5: Photograph of the outdoor setting: a 12 m × 11.6 m area. A red and white ribbon grid defines a mesh of 870 square subelements with 40 cm edge.

from which we recover the known wave-equation, as well as we can argue relatively very high average time to get a decision. Indeed, there is not sufficient time for the stochastic process to diffuse. As a consequence, it is apparent an intimate relationship between *time* and *flow* in our model. Although the two subcategories are conceptually different, urgency or rushing [16] are generally competitors of careful actions.

Finally, in our description, the *flow* is related to a sort of memory of the motion, of the previous sequence of foot movements. A relatively bound *flow* is expected to be associated with a smaller stochastic component $\mathbf{v}_r$, but, in some cases, it can be perceived by the observer as also associated with a longer average time for taking a decision. A random walker that keeps the memory of the previous steps is known in the literature as a persistent random walker [26], which corresponds, in our case, to a relatively γ small value.

4. Experimental Analysis

A preliminary experimental analysis was carried out to observe the walk trajectories associated with different combinations of the *Effort* four subcategories. In Fig. 5, a photograph of the prepared outdoor setting is shown. A 12 m × 11.6 m meshed area was divided into 870 square subelements of 40 cm edge each, which is the adopted spatial resolution in our estimation of the step position and observed spatial trajectory. We chose an outdoor setting with such dimensions to prevent as much as possible from the border effect. Indeed, too much small space constrains the trajectories and limits the efficacy of the analysis. Based on the obtained results, the chosen dimensions are an acceptable compromise for the present purposes. Besides, the experiment occurred in an open countryside in late springtime. The participants walked on a meadow with short grass, and we did not register particularly evident visuals, olfactory and audial stimuli to which they could react.

We did not apply any sensors to the volunteers during the campaign, and we acquired videos of their walks with a commercial video camera. The time resolution of the video camera was about 33 ms. Because of the

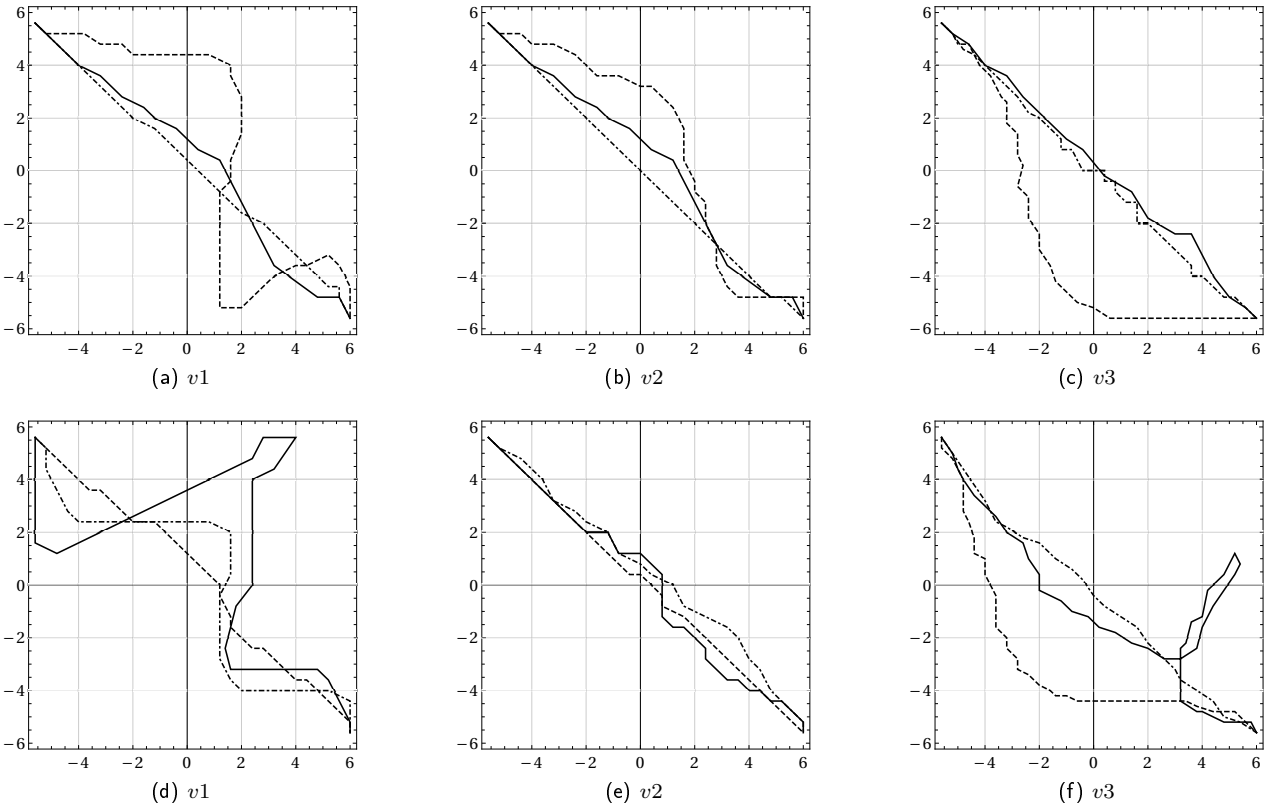

Figure 6: Upper panel trajectories: direct *space*-sudden *time* (solid line), -sustained *time* (dashed line) and -bound *flow* (dash-dotted line), (a) $v1$; (b) $v2$; (c) $v3$. Lower panel trajectories: direct *space*-free *flow* (solid line), -heavy *weight* (dashed line), and -light *weight* (dash-dotted line), (d) $v1$; (e) $v2$; (f) $v3$.

limited statistics, we did not report any sex or age classification. Thus, the volunteers are here identified simply as $v1$, $v2$, ..., $v5$.

All the volunteers had no specialized training, and they were not informed about our model framework. They all received the same input for a direct *space*: start the movement from a vertex of the square ($x = -6$ m, $y = 6$ m), and finally, exit the setting from the opposite vertex ($x = 6$ m, $y = -5.6$ m). Then, prior the videorecording of each of the six walk combinations with the other three subcategories, *time*, *flow* and *weight*, each walker received the same following inputs: for a sudden *time* - "imagine you are in a hurry"; for a sustained *time* - "imagine you have ample time available"; for a bound *flow* - "imagine you are carrying a cup of tea"; for a free *flow* - "imagine you are a joyful child"; for a heavy *weight* - "imagine you are burdened with a heavy load"; for a light *weight* - "imagine you are floating in the air".

All the walkers clearly understood the context and intended situation. Each walker performed the six combinations individually. They received no other inputs and no constraints on their performance time, leaving them as much as possible free to interpret their movement.

The observed trajectories are reported in Fig. 6: dimensions are in (m). The upper plots refer to the combined direct *space*-sudden *time* (solid line), -sustained *time* (dashed line), and -bound *flow* (dash-dotted line); the lower figures show the trajectories in association with free *flow* (solid line), heavy *weight* (dashed line), and light *weight* (dash-dotted line). From left to right, the panels refer to $v1$, $v2$, $v3$. The analogous trajectories to Fig. 6, are shown in Fig. 7 for $v4$ and $v5$. For the sake of readability, the combined case, direct *space*-light *weight*, is shown separately for both $v4$ and $v5$ (right subplots (c) and (f), respectively).

For all the volunteers, results mostly show how the trajectories relevant to sustained *time*, free *flow*, and light *weight* are more dispersed over the square, compared to their counterparts, which show paths much tight closer to the diagonal.

5. Random Time Analysis

As discussed in Sec. 3, the waiting time distribution $\psi(t)$ represents the distribution of the random times at which the random walk movement changes. An accurate description of what identifies a movement change is a key question for properly defining our subject of investigation. In this Section, we further clarify how to get the random step and velocity components and

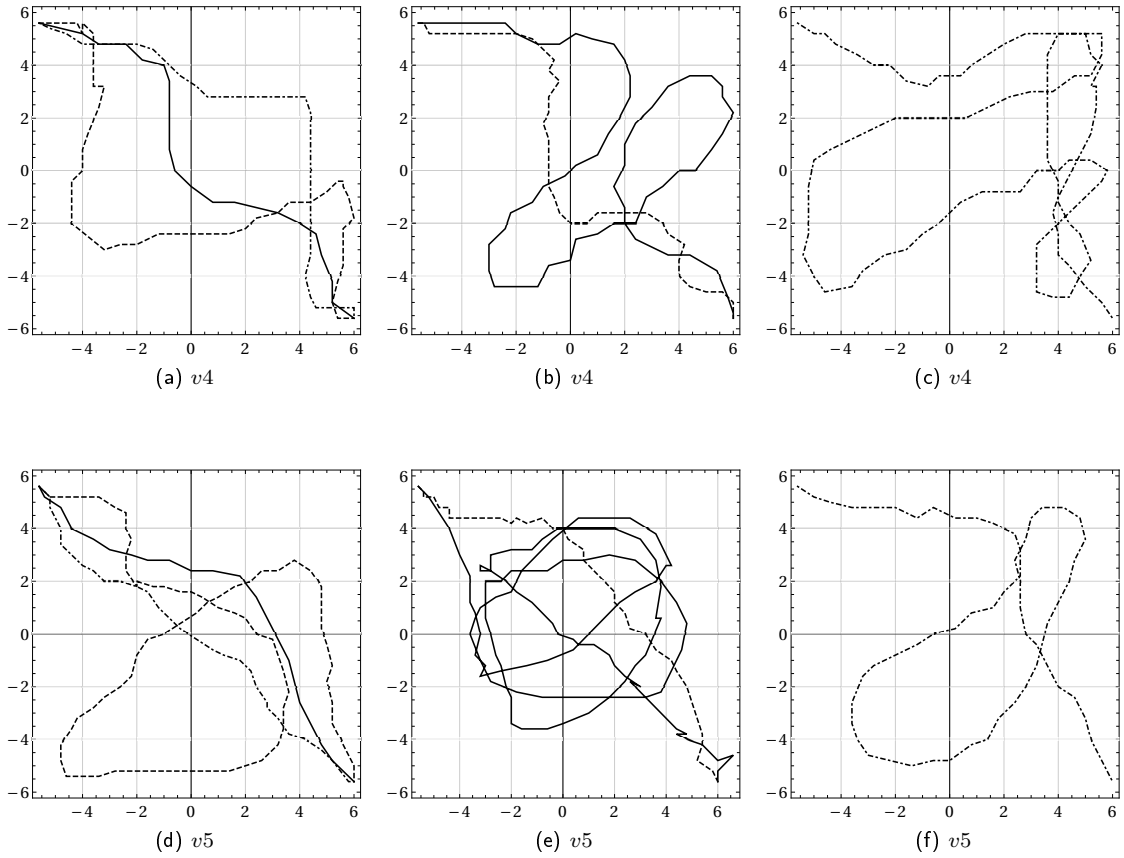

Figure 7: Upper panel trajectories ($v4$): (a) direct *space*-sudden *time* (solid line), -sustained *time* (dashed line) and -bound *flow* (dash-dotted line); (b) direct *space*-free *flow* (solid line), -heavy *weight* (dashed line); (c) direct *space*-light *weight* (dash-dotted line). The analogous trajectories of $v5$ are shown in the lower panels (d), (e) and (f).

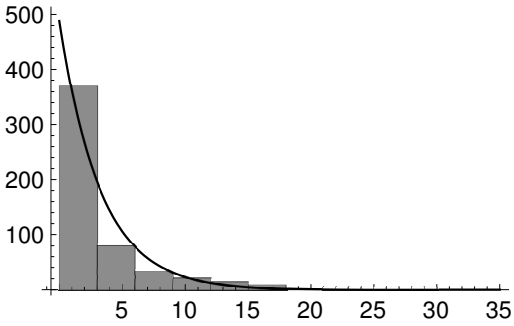

Figure 8: Reconstructed waiting time distribution for a virtual character, histogram. Obtained exponential distribution (solid line) with the exponential term $\gamma = 0.305$ s^{-1}.

the random times from the measurements reported in Sec. 4. For each subcategory case, we thus combined the data relevant to all the five volunteers to form a single data sheet. Then, we determined the two mean components of the term $\mathbf{v}_d$ of (3) by dividing the total length along x and y by the exit time. It is worth remarking that $v_{dx} \sim v_{dy}$ for all the tests. To get the random components of $\mathbf{v}_r$, we then proceeded as follows: firstly, we subtracted the average step length from the actual step length, thus obtaining the random step component; next, at each time of observation, i.e., at each step, we divided the random step by the time duration of the step, thus obtaining the random velocity; finally, we got the average of the absolute values of the random components $v_{rx} \sim v_{ry}$.

In particular, we got larger $\mathbf{v}_r$ components for the combined direct *space*-sudden *time*, -free *flow*, and -light *weight* subcategories, compared with their counterparts.

In Fig. 8, we show the waiting time distributions of a virtual character reconstructed from the random time distributions of all five volunteers. Time intervals, i.e., the random times, are those at which $\mathbf{v}_r$ changes its sign, while the parameter $\gamma = 0.305$ s^{-1} is evaluated as the inverse of the average time interval. In particular, we can observe a substantial agreement with the assumption of an exponential distribution, solid line curve.

In Tab. 1, we summarize the experimental parameters relevant to the considered combinations of the *Effort* subcategories. Results show a relatively shorter mean time interval ($1/\gamma = 1.2$ s) for the direct *space*-sudden *time* performance, while for all the other cases, average time intervals are approximately between 3 s

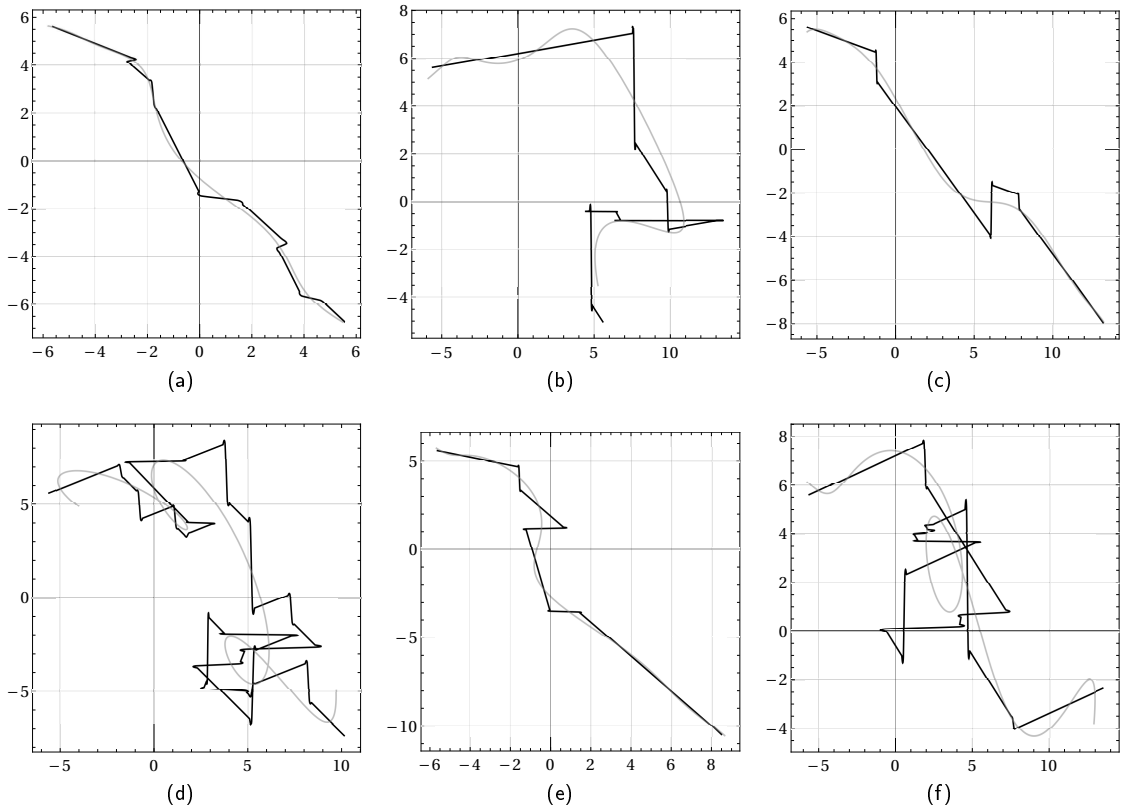

Figure 9: Simulated trajectories. From left to right: (upper panels) direct *space*-sudden *time*, -sustained *time*, -bound *flow*; (lower panels) -free *flow*, -heavy *weight*, -light *weight*.

Table 1
Experimental parameters identified from the observed trajectories; v_d stands for $v_{dx} \sim v_{dy}$, v_r for $v_{rx} \sim v_{ry}$, respectively. Reported subcategories are combined with a direct *space*.

	$1/\gamma$ (s)	v_d (m/s)	v_r (m/s)
sudden *time*	1.22	1.33	0.52
sustained *time*	3.75	0.31	0.40
bound *flow*	3.17	0.31	0.20
free *flow*	3.17	0.34	0.90
heavy *weight*	3.90	0.30	0.19
light *weight*	4.05	0.35	0.66

and 4 s. Furthermore, higher $\mathbf{v}_r$ appear for the combined direct *space*-free *flow* and -light *weight* compared to their counterparts.

6. Simulation Results

In this Section, we simulate the trajectory of a virtual random walker. As we will show the results are promising, and, in principle, the model can be extended to simulate more complex movements.

In Fig. 9, typical simulated trajectories, in a statistical sense are shown for all the considered cases. At first glance, the results show a clear difference for the combined subcategories direct *space*-sudden *time*, -bound *flow*, and -heavy *weight*, compared with the other cases, and they appear in substantial agreement with the observed trajectories of the five volunteers. It is important to point out that the agreement has to be intended in a statistical sense.

It is possible to notice how the simulated trajectories show abrupt changes in direction (formation of tip points). However, this is not an intrinsic limit of the model but just a consequence of the adopted approximations in the current version. An underlined gray fit line is also reported to help the reading of the simulated paths.

Besides, it is worth noting that the simulated combinations of direct *space*-sudden *time*, -bound *flow*, and -heavy *weight* also exhibit trajectories that are relatively close to a straight line. Such trajectories show a substantial statistical agreement with the trajectories displayed by the five volunteers in Fig. 6 and Fig. 7 for the corresponding combinations. In the case of the volunteers' trajectories, they also tend to be generally close to a straight line.

Furthermore, the simulated direct *space*-sustained *time*, -free *flow*, and -light *weight*, all express more sense of indulgence in the space, i.e., more occupancy of the area as a result of a higher stochastic component

relatively to the intensities of the other two parameters γ and $\mathbf{v}_d$. Besides, the observer perceives less possibility of repeating the very same sequence for the simulated sustained *time*, free *flow*, and light *weight*. This can find, for example, confirmation, if we imagine observing a healthy adult or a little child, both attracted by a deterministic force toward an objective. Both the adult and the little child will define a trajectory, but it is expected that if they are asked to repeat their movement, the little child should deviate more evidently from its previous path.

7. Conclusion

We analyzed the human walk via a combined deterministic-stochastic model based on a random walk framework. Along with the Laban Movement Analysis, we recalled the main features of the four *Effort* subcategories, and combined deterministic and stochastic forces to represent the movement qualities associated with the Laban *space*, *weight*, *time*, and *flow*. As a major aspect of our discussion, we pointed out how the time distribution has a central role in the model characterizing the randomly extracted instants when the walk movement changes. We then reported the results of an experimental analysis performed in an outdoor setting with volunteers walking on a plane. In particular, we included the trajectories performed by five volunteers as a result of different combinations of a direct *space* with the other subcategories. Furthermore, we discussed the identification process of the model parameters from the measured trajectories, and we presented the outputs of our model via randomly extracted trajectories of a virtual character. The obtained results showed a substantial agreement with the observed trajectories and encourage to further investigate the presented approach based on statistical quantities to analyze the human walks associated with different combinations of the Laban *Effort* subcategories.

References

[1] T. K. Uchida, A. Seth, Conclusion or illusion: Quantifying uncertainty in inverse analyses from marker-based motion capture due to errors in marker registration and model scaling, Frontiers in Bioengineering and Biotechnology 10 (874725) (2022) 1–11.

[2] A. Cappozzo, U. D. Croce, Human movement analysis using stereophotogrammetry - part 1: theoretical background, Gait and Posture 21 (2005) 186–196.

[3] A. Ancillao, Analysis and measurement of human motion: Modern protocols and clinical considerations, Journal of Mechanical Engineering and Robotics Research 1 (4) (2016) 30–37.

[4] E. Irzmańska, T. Tokarski, Human movement analysis in evaluation of the risk of falls in younger and older workers while wearing protective footwear, Measurement 91 (2016) 19–24.

[5] D. Pan, H. Liu, Human falling recognition based on movement energy expenditure feature, Hindawi 2021 (2021) 1–12.

[6] H. N. Falch, H. G. Rædergàard, R. Tillaar, Effect of approach distance and change of direction angles upon step and joint kinematics, peak muscle activation, and change of direction performance, Frontiers in Sports and Active Living 2 (2020) 1–10.

[7] L. L. Raket, B. Grimme, G. Schöner, C. Igel, B. Markussen, Separating timing, movement conditions and individual differences in the analysis of human movement, Plos Computational Biology (1005092) (2016) 1–27.

[8] S. Manitsaris, G. Senteri, D. Makrygiannis, A. Glushkova, Human movement representation on multivariate time series for recognition of professional gestures and forecasting their trajectories, Frontiers in Robotics and AI 7 (80) (2022) 1–20.

[9] W. Ding, Z. Cao, J. Zhang, R. Chen, X. Guo, G. Wang, Radar-based 3d human skeleton estimation by kinematic constrained learning, IEEE Sensors Journal 21 (20) (2021) 23174–23184.

[10] L. Zhou, N. Lanna, G. Fan, Joint optimization of kinematics and anthropometrics for human motion denoising, IEEE Sensors Journal 22 (5) (2022) 4386–4399.

[11] V. Medved, Measurement and Analysis of Human Locomotion, Springer Nature, Cham Switzerland, 2021.

[12] M. Karg, A.-A. Samadami, R. Gorbet, K. Kühnlenz, J. Hoey, D. Kulić, Body movements for affective expression: A survey of automatic recognition and generation, IEEE Transactions on Affective Computing 4 (4) (2013) 341–359.

[13] J. Rett, J. Dias, J.-M. Ahuactzin, Laban movement analysis using a bayesian model and perspective projections, in: C. Rossi (Ed.), Brain, Vision and AI, IntechOpen, Rijeka, 2008, pp. 183–210.

[14] D. Swaminathan, H. Thornburg, J. Mumford, S. Rajko, J. James, T. Ingalls, E. Campana, G. Qian, P. Sampath, B. Peng, A dynamic bayesian approach to computational laban shape quality analysis, Advances in Human-Computer Interaction 2009 (362651) (2009) 1–17.

[15] R. Laban, The Mastery of Movement, MacDonald and Evans Ltd, London, 1960.

[16] I. Bartenieff, D. Lewis, Body Movement: Coping With the Environment, Gordon and Breach Science Pub., New York, 1980.

[17] R. P. Tsachor, T. Shafir, A somatic movement approach to fostering emotional resiliency through laban movement analysis, Frontiers in Human Neuroscience 11 (410) (2017) 1–8.

[18] M. Davis, Effort-shape analysis: evaluation of its logic and consistency and its systematic use in research, in: I. Bartenieff, M. Davis, F. Paulay (Eds.), Four Adaptations of Effort Theory in Research and Teaching, Dance Notation Bureau, New York, 1970.

[19] T. Kawano, Developing a dance movement therapy approach to qualitatively analyzing interview data, The Arts in Psychotherapy 56 (–) (2017) 61–73.

[20] A. Foroud, I. Q. Whishaw, Changes in the kinematic structure and non-kinematic features of movements during skilled reaching after stroke: A laban movement analysis in two case studies, Journal of Neuroscience Methods 158 (1) (2006) 137–149.

[21] L. C. dos Santos, Laban Movement Analysis: A Bayesian Computational Approach to Hierarchical Motion Analysis and Learning, PhD Dissertation, University of Coimbra, Coimbra, Portugal, 2014.

[22] A. Melzer, T. Shafir, R. P. Tsachor, How do we recognize emotion from movement? specific motor components contribute to the recognition of each emotion, Frontiers in Psycholoty 10 (–) (2019) 1–14.

[23] E. W. Montroll, G. H. Weiss, Random walks on lattices. ii, Journal of Mathematical Physics 6 (2) (1965) 167–181.

[24] R. Kubo, M. Toda, N. Hashitsume, Statistical Physics II Nonequilibrium Statistical Mechanics, Springer-Verlag, Berlin Heidelberg, 1985.
[25] G. Zumofen, J. Klafter, Scale-invariant motion in intermittent chaotic systems, Physical Review E 47 (2) (1993) 851–863.
[26] G. H. Weiss, Aspects and Applications of the Random Walk, North Holland, Amsterdam, 1994.
[27] M. Smoluchowski, Drei vorträge über diffusion brownsche bewegung and koagulation von kolloidteilchen, Gordon and Breach Science Pub., New York, 1980.
[28] M. Smoluchowski, Marian Smoluchowski. Selected Scientific Works, Wydawnictwa Uniwersytetu Warszawskiego, Warszawa, 2017.